Analysis of Topological Material Surfaces

Taro Kimura

Abstract

We provide a systematic analysis of the boundary condition for the edge state, which is a ubiquitous feature in topological phases of matter. We show how to characterize the boundary condition, and how the edge state spectrum depends on it, with several examples, including 2d topological insulator and 3d Weyl semimetal. We also demonstrate the edge-of-edge state localized at the intersection of boundaries.

Keywords: topological insulator, Weyl semimetal, boundary condition, lattice fermion

1. Introduction

Study of topological phases of matter has been a hot topic in condensed-matter physics for recent years [1]. An importance of topological aspects of materials themselves was already noticed around the discovery of quantum Hall effect (QHE) in early 1980s. QHE is universally observed in a two-dimensional system, but it requires a strong magnetic field, which breaks time-reversal symmetry. A breakthrough after 20 years was the discovery of quantum spin Hall effect (QSHE), which actually demonstrates that a topological phase is possible even without breaking time-reversal symmetry. This opens a new window of the research on topological insulators (TIs) and topological superconductors (TSCs).

A universal feature of topological phases is the bulk/edge correspondence [2]: once the bulk wave function has a topologically nontrivial configuration; there exists a gapless edge state

localized at the boundary. Such an edge state is topologically protected, and thus is robust against any perturbations as long as respecting symmetry of the system. In practice, the edge state plays a significant role in detection of topological phases since it can be directly observed in experiments using angle-resolved photo-emission spectroscopy (ARPES). Therefore the boundary condition dependence of the edge state is expected to provide experimentally useful predictions.

In this article, we provide a systematic analysis of the boundary condition of topological material surfaces, including TIs and also Weyl semimetals (WSMs) [3, 4].[1] In Section 2, we discuss some preliminaries on the band topology of TI and WSM. We explain how one can obtain topological invariants from the band spectrum. In Section 3, we provide a systematic study of the boundary condition. We show how to obtain and characterize the boundary condition for a given Lagrangian or Hamiltonian. Then we apply this analysis to the edge state of 2d TI and 3d WSM both in the continuum effective model and the discretized lattice model. In Section 4, we extend the analysis to the situation with two boundaries in different directions. We demonstrate the existence of the edge state localized at the intersection of surfaces, that we call the edge-of-edge state.

2. Preliminaries: bulk, edge, and topology

In this section, we provide several preliminary aspects of topological materials. In particular, we show simple models, effectively describing the bulk of topological system, and discuss the role of topology thereof.

2.1. Bulk system

We start with a simple two-band Hamiltonian in two dimensions,

$$H_{2d} = -i\sigma_1 \frac{\partial}{\partial x_1} - i\sigma_2 \frac{\partial}{\partial x_2} + m\sigma_3 \tag{1}$$

where Pauli matrices are defined $\sigma_1 = \begin{pmatrix} 0 & 1 \\ 1 & 0 \end{pmatrix}$, $\sigma_2 = \begin{pmatrix} 0 & -i \\ i & 0 \end{pmatrix}$, $\sigma_3 = \begin{pmatrix} 1 & 0 \\ 0 & -1 \end{pmatrix}$. This is a simple effective model for 2d Integer QHE, classified into the 2d class A system according to the 10-fold way classification of TIs and TSCs [8, 9]. In order to investigate the band structure of this system, we consider the Bloch wave function $\Psi_{\vec{p}}(\vec{x}) = e^{i\vec{p}\cdot\vec{x}}\psi_{\vec{p}}(\vec{x})$, and the corresponding Hamiltonian acting on $\psi_{\vec{p}}(\vec{x})$, simply denoted by ψ below, is given by

---

[1]See also related works [5–7] for the boundary condition analysis of topological materials.

$$\mathcal{H}_{2d}\left(\vec{p}\right) = p_1\sigma_1 + p_2\sigma_2 + m\sigma_3 = \begin{pmatrix} m & \Delta^*\left(\vec{p}\right) \\ \Delta\left(\vec{p}\right) & -m \end{pmatrix}. \tag{2}$$

We obtain two eigenvalues $\epsilon_{\pm}\left(\vec{p}\right) = \pm\sqrt{\left|\vec{p}\right|^2 + m^2}$. The eigenstate, parametrized by a complex number $\xi \in \mathbb{C}$, is accordingly obtained as

$$\psi = \frac{1}{\sqrt{1 + |\xi|^2}}\begin{pmatrix} 1 \\ \xi \end{pmatrix} \quad \text{with} \quad \xi = \frac{\Delta\left(\vec{p}\right)}{\epsilon + m} = \frac{\epsilon - m}{\Delta\left(\vec{p}\right)^*}. \tag{3}$$

We remark that the parameter ξ becomes singular $\xi \to \infty$ at $\vec{p} = 0$. At this point, we have to reparametrize the eigenstate with ξ^{-1} instead of ξ. This means that ξ is not a global, but just a local coordinate, and the eigenstate is given by an element of $\mathbb{C}\mathbf{P}^1$ in this model.

Since this system is gapped, we can neglect the transition between lower and upper bands as long as we consider the adiabatic process. Under such a process, we can consider the Berry connection and curvature defined from the gapped eigenstate[2]

$$\mathcal{A} = \psi^{\dagger}(id)\psi = -\text{Im}\frac{\xi^* d\xi}{1 + |\xi|^2}, \qquad \mathcal{F} = d\mathcal{A} = i\frac{d\xi^* d\xi}{\left(1 + |\xi|^2\right)^2} \tag{4}$$

where we use the differential form notation in the momentum space, $d = \left(\partial/\partial p_i\right)dp^i$, namely the Berry connection is one-form $\mathcal{A} = A_1 dp^1 + A_2 dp^2$, and the curvature is two-form $\mathcal{F} = F_{12}dp^1 dp^2$. Under the momentum-dependent transformation, $\xi \to e^{i\phi(\vec{p})}\xi$ (not an overall phase rotation of the eigenstate ψ), the connection behaves as $\mathcal{A} \to \mathcal{A} - d\phi/\left(1 + |\xi|^2\right)$. This is a U(1) gauge transformation, which is local in momentum space, and the curvature is invariant under this transformation by itself. This U(1) structure is directly related to the S^1 fibration of $\mathbb{C}\mathbf{P}^1 = S^3/S^1$, and interpreted as a consequence of the particle number conservation of each eigenstate which holds under the adiabatic process.

An important point is that we can construct the topological invariant from the Berry connection and curvature (4). For the 2d system, it is given as an integral of the curvature over the momentum space,

$$\nu_{2d} = \frac{1}{2\pi}\int dp_1 dp_2 \, F_{12} = \frac{1}{2}\,\text{sgn}\left(m\right) \tag{5}$$

which is called the TKNN number, which computes the Hall conductivity of the system [11]. We remark that it is invariant under the continuous deformation of the mass parameter, so that

---

[2]See a textbook on this topic, e.g., [10] for more details.

it would be a topological invariant, but with a discontinuous point at $m = 0$, which is the gapless (sign changing) point $m = 0$. Typically the topological number takes an integer value, but v_{2d} does not. The reason why we obtain a half integer value is that we take a specific slice of the mass parameter in the total parameter space of the three-parameter Hamiltonian (2).

To explain this let us consider the 3d system as follows,

$$\mathcal{H}_{3d}\left(\vec{p}\right) = p_1\sigma_1 + p_2\sigma_2 + p_3\sigma_3 = \begin{pmatrix} p_3 & \Delta^*(p) \\ \Delta(p) & -p_3 \end{pmatrix} \tag{6}$$

which is known as an effective Hamiltonian of the WSM. This Hamiltonian is simply obtained from the 2d system (2) by replacing the mass parameter with another momentum p_3. We apply essentially the same analysis to this 3d system as 2d, and we obtain the genuine topological invariant:

$$v_{3d} = \frac{1}{4\pi}\int_{S^2} d\,\vec{S}\cdot\vec{B} = \frac{1}{2\pi}\int dp_1 dp_2\, F_{12}\Big|_{p_3>0} - \frac{1}{2\pi}\int dp_1 dp_2\, F_{12}\Big|_{p_3<0} = 1 \tag{7}$$

where the "magnetic field" is defined as $B^i = \frac{1}{2}\epsilon^{ijk}F_{jk}$, namely $\vec{B} = \vec{\nabla}\times\vec{A}$. This means that the gapless point (also called the Weyl point) plays a role as the magnetic monopole in the momentum space. As shown in **Figure 1**, the 2d invariant v_{2d} is related to the 3d invariant through taking a constant p_3, identified with the mass m, which covers either upper or lower half of the monopole fluxes. This explains why the 2d invariant can be a half-integer, although the 3d invariant takes an integer value. We remark that, in this case, one cannot consider well-defined Berry phase, since the current 3d system is gapless in which the adiabatic process does not make sense. However, the topological invariant still plays a role to discuss stability of the Weyl point: Since a system having a nontrivial topological number, say $v_{3d} \neq 0$, cannot be
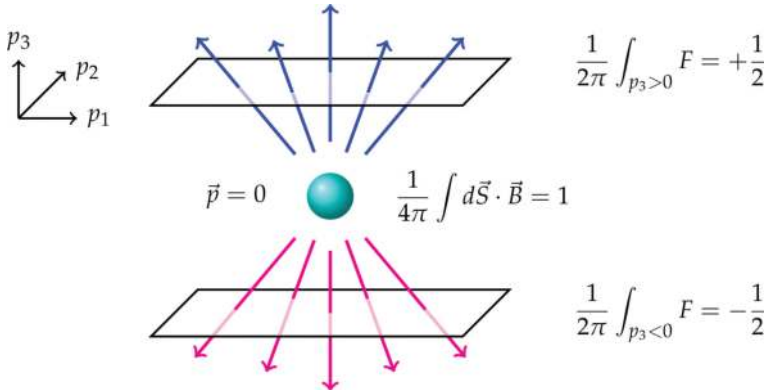

Figure 1. Monopole at Weyl point in the momentum space. The monopole charge is an integer-valued topological invariant v_{3d}. The 2d invariant v_{2d} is obtained at a constant $p_3(\to m)$ plane, which covers either upper or lower half of the fluxes, so that v_{2d} is given by a half of v_{3d}.

continuously deformed to a trivial system $\nu_{3d} = 0$ by definition. This explains the topological stability of the WSM. If we want to obtain a topologically trivial situation, we need pair-annihilation of the Weyl points having opposite topological invariants: $\nu_{3d} = (+1) + (-1) = 0$. See **Figure 2**.

2.2. Edge state

So far, we have discussed the bulk system, and the material boundary is not yet considered. Let us show a simple argument to incorporate the boundary of the system. If we have a material which has nontrivial topology, the vacuum, outside of the material, should be topologically trivial. Otherwise they cannot be topologically distinguished. As explained above, in order to obtain the topology change in the 2d system, we need the mass parameter whose sign is flipped at the boundary. For this purpose we impose a simple spatial dependence on the mass parameter as $m(x_1) = \vartheta x_1$ with a positive slope $\vartheta > 0$, giving rise to the sign flip at $x_1 = 0$, so that the boundary is the plane $x_1 = 0$ [12]. Then the Hamiltonian takes a form of

$$\mathscr{H}_{2d}(x_1, p_2) = m(x_1)\sigma_1 - i\sigma_2 \frac{\partial}{\partial x_1} + p_2\sigma_3 = \begin{pmatrix} p_2 & \sqrt{2\vartheta}\,\hat{a}^\dagger \\ \sqrt{2\vartheta}\,\hat{a} & -p_2 \end{pmatrix} \qquad (8)$$

where we exchange Pauli matrices compared with the previous one to simplify the expression. Since x_1-dependence remains in this system, we do not consider the momentum basis in x_1-direction, while the momentum in x_2-direction is now denoted by p_2. The off-diagonal element is given by an operator $\hat{a} = (\vartheta x_1 + (\partial/\partial x_1))/\sqrt{2\vartheta}$, $\hat{a}^\dagger = (\vartheta x_1 - (\partial/\partial x_1))/\sqrt{2\vartheta}$, obeying the commutation relation $\left[\hat{a}, \hat{a}^\dagger\right] = 1$, so that it is interpreted as a creation/annihilation operator. Then the energy spectrum is given by $\epsilon_n(p_2) = \pm\sqrt{p_2^2 + 2\vartheta n}$ for $n \geq 1$ (gapped), while the zero mode dispersion is given by $\epsilon_0(p_2) = p_2$ (gapless), which is the chiral edge state of the 2d class A system. See **Figure 3** for numerical plot of the spectrum. In general, we obtain the zero mode localized on the topological material boundary from the mass term
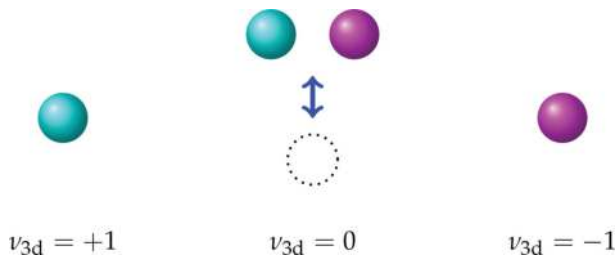

$$\nu_{3d} = +1 \qquad\qquad \nu_{3d} = 0 \qquad\qquad \nu_{3d} = -1$$

Figure 2. The topological invariant distinguishes topologically different situations. The green and red spheres show the monopole with topological charge $\nu_{3d} = +1$ and $\nu_{3d} = -1$, respectively. We need pair annihilation to eliminate the monopoles.
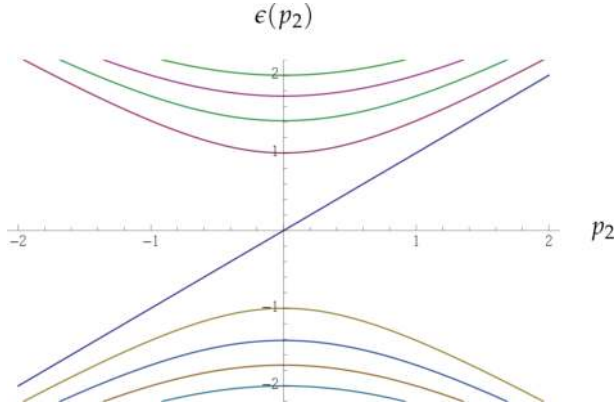
$$\epsilon(p_2)$$

Figure 3. The dispersion relation of the edge state with $\vartheta = 1$. We find a gapless chiral mode specific to the 2d class A TI. The gapped spectra are interpreted as bulk contributions.

with a spatial profile, which is known as the domain-wall fermion. See, for example, [13] for more details.

2.3. Lattice system

Since the electron lives on a lattice in the material, studying the lattice model is important to understand the actual behavior of the electron. Let us introduce the Hamiltonian describing the electron on a lattice

$$H_{2d}^{\text{lat}} = -\frac{i}{2}\sigma_1\left(\nabla_1 - \nabla_1^\dagger\right) - \frac{i}{2}\sigma_2\left(\nabla_2 - \nabla_2^\dagger\right) + \sigma_3\left(m + 2 - \frac{1}{2}\left(\nabla_1 + \nabla_1^\dagger\right) - \frac{1}{2}\left(\nabla_2 + \nabla_2^\dagger\right)\right) \quad (9)$$

where we define the difference operator $\nabla_{1,2}\psi_{\vec{n}} = \psi_{\vec{n}+\vec{e}_{1,2}} - \psi_{\vec{n}}$ with the unit vector $\vec{e}_{1,2}$ in n_1 and n_2-direction. Then the corresponding Bloch Hamiltonian is given by

$$\mathcal{H}_{2d}^{\text{lat}}\left(\vec{p}\right) = \sigma_1 \sin p_1 + \sigma_2 \sin p_2 + \sigma_3\left(m + 2 - \cos p_1 - \cos p_2\right). \quad (10)$$

Periodicity $p_{1,2} \sim p_{1,2} + 2\pi$ reflects the lattice structure: The momentum is restricted to the Brillouin zone $p_{1,2} \in [0, 2\pi]$. The spectrum is given by $\epsilon\left(\vec{p}\right) = \pm\sqrt{\left(\sin p_1\right)^2 + \left(\sin p_2\right)^2 + \left(m + 2 - \cos p_1 - \cos p_2\right)^2}$, which has four gapless points $\vec{p} = (0,0)$ at $m = 0$, $\vec{p} = (\pi, 0)$ and $(0, \pi)$ at $m = -2$, $\vec{p} = (\pi, \pi)$ at $m = -4$. Expanding the momentum around $\vec{p} = (0,0)$, one can see the effective Hamiltonian (2) is obtained. If expanding the momentum around $\vec{p} = (\pi, 0)$ instead, we similarly obtain the Hamiltonian (2), but we have to replace $p_1 \rightarrow -p_1$.
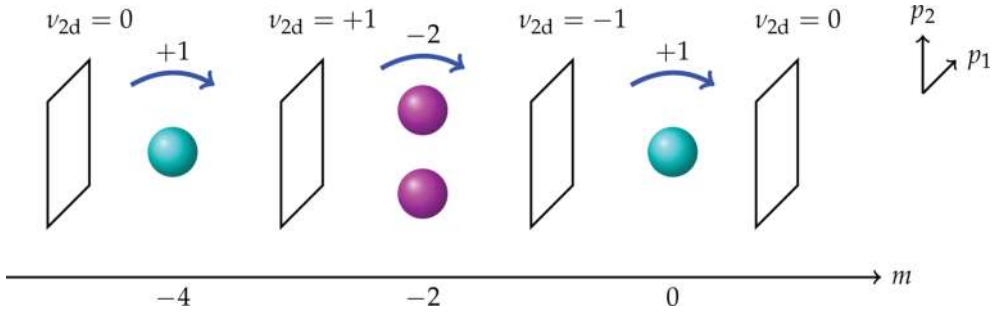
Figure 4. The mass dependence of the 2d topological invariant v_{2d} for the lattice model (10). Topology change occurs at the gapless points $m = -4, -2, 0$. Change of the invariant corresponds to the monopole charge $+1, -2, +1$ associated with each gapless point.

Let us see the topological structure of the lattice model. Applying the same procedure to the Hamiltonian (10), we obtain the topological invariant as follows [14]:

$$v_{2d} = \frac{1}{2\pi} \int_{BZ} dp_1 dp_2 \, F_{12} = \begin{cases} 0 & (m > 0 \text{ or } m < -4) \\ -1 & (-2 < m < 0) \\ +1 & (-4 < m < -2) \end{cases} \tag{11}$$

where the momentum integral is taken over the Brillouin zone. In contrast to the continuum effective model, we have integer valued topological invariants in this case. This is essentially related to the anomaly of (2 + 1)-dimensional Dirac system, known as the parity anomaly. However, it is also known that the lattice regularization naively gives rise to an anomaly-free system: The gapless points have to appear as a pair, so that each anomalous contribution is canceled with each other [15, 16]. Actually the present model (10) has four gapless points in the parameter space: $(p_1, p_2, m) = (0,0,0), (\pi,0,-2), (0,\pi,-2), (\pi,\pi,-4)$. Each gapless point plays basically the same role as that discussed in the continuum model with the monopole charge $+1$ or -1. Thus we immediately obtain $v_{2d} = \frac{1}{2}(+1 - 2 + 1) = 0$ for $m > 0$, $\frac{1}{2}(-1 - 2 + 1) = 1$ for $-2 < m < 0$, $\frac{1}{2}(-1 + 2 + 1) = 1$ for $-4 < m < -2$, and $\frac{1}{2}(-1 + 2 - 1) = 0$ for $m < -4$. See **Figure 4**.

We can similarly consider a lattice model for 3d WSM system. We consider the Hamiltonian defined on a 3d lattice

$$H_{3d}^{lat} = \frac{1}{2}\sigma_1\left(\nabla_1 + \nabla_1^\dagger - \nabla_2 - \nabla_2^\dagger + 2c\right) - \frac{i}{2}\sigma_2\left(\nabla_2 - \nabla_2^\dagger\right) - \frac{i}{2}\sigma_3\left(\nabla_3 - \nabla_3^\dagger\right). \tag{12}$$

The corresponding Bloch Hamiltonian is given by

$$\mathcal{H}_{3d}^{lat}\left(\vec{p}\right) = \sigma_1\left(\cos p_1 - \cos p_2 + c\right) + \sigma_2 \sin p_2 + \sigma_3 \sin p_3, \tag{13}$$

and the spectrum yields $\epsilon\left(\vec{p}\right) = \pm\sqrt{\left(\cos p_1 - \cos p_2 + c\right)^2 + \left(\sin p_2\right)^2 + \left(\sin p_3\right)^2}$. The parameter c tunes the gapless Weyl points as follows

$$(p_1, p_2, p_3) = \begin{cases} \left(\cos^{-1}(1-c), 0, 0\right) \ \& \ \left(\cos^{-1}(1+c), 0, \pi\right) & (0 < c < 2) \\ \left(\cos^{-1}(-1-c), \pi, 0\right) \ \& \ \left(\cos^{-1}(1+c), \pi, \pi\right) & (-2 < c < 0) \\ \text{n/a} & (|c| > 2) \end{cases} \tag{14}$$

The band spectrum is shown in **Figure 5** at $p_3 = 0$ and $c = 1$. We can see two Weyl points at $(p_1, p_2) = (\pm\pi/2, 0)$. We will study the boundary condition of this model in Section 3.3.

2.4. Higher-dimensional system

So far we have considered a simple system in two and three dimensions. We can even discuss such a topological structure in the momentum space of more involved systems. In this section we discuss a higher-dimensional generalization of the system discussed above. Dimensional reduction of this system gives rise to several interesting situations in 2d and 3d.

We consider a four-band model defined in four spatial dimensions, which is a natural higher-dimensional generalization of (2),

$$\mathcal{H}_{4d}(p) = p \cdot \gamma + m\gamma_5 = \begin{pmatrix} m & \Delta(p)^\dagger \\ \Delta(p) & -m \end{pmatrix} \quad \text{with} \quad \Delta(p) = p \cdot \sigma = \begin{pmatrix} p_4 + ip_3 & p_2 + ip_1 \\ -p_2 + ip_1 & p_4 - ip_3 \end{pmatrix} \tag{15}$$

where we use the gamma matrices defined as $\gamma_k = \begin{pmatrix} 0 & -i\sigma_k \\ \sigma_k & 0 \end{pmatrix}$ for $k = 1, 2, 3$, $\gamma_4 = \begin{pmatrix} 0 & \mathbb{1} \\ \mathbb{1} & 0 \end{pmatrix}$,
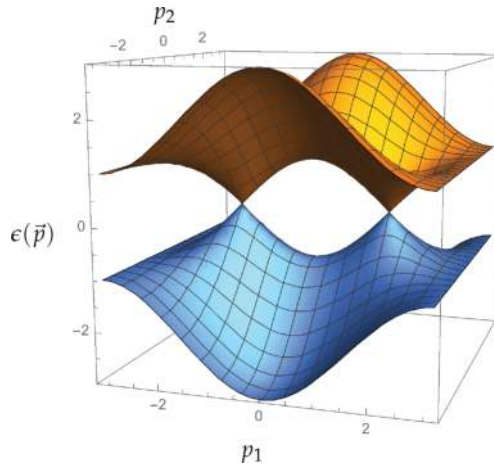

Figure 5. The energy spectrum of the lattice WSM model (13) with $p_3 = 0$ and $c = 1$. There exist two gapless Weyl points at $(p_1, p_2) = (\pm\pi/2, 0)$. The parameter c characterizes the distance between the Weyl points.

$\gamma_5 = \begin{pmatrix} \mathbb{1} & 0 \\ 0 & -\mathbb{1} \end{pmatrix}$, and the off-diagonal element is given by $\Delta(p) = p \cdot \sigma \in \mathbb{H}$ with $\sigma = \left(i \, \vec{\sigma}, \mathbb{1} \right)$. We remark that this Hamiltonian is a 4×4 matrix, such that each element shows a 2×2 matrix. The spectrum is simply obtained as $\epsilon(p) = \pm \sqrt{|p|^2 + m^2}$, and each state is doubly degenerated. We have a similar eigenvector to (3) as follows,

$$\psi = \frac{1}{\sqrt{1 + |\xi|^2}} \begin{pmatrix} \mathbb{1} \\ \xi \end{pmatrix} \quad \text{with} \quad \xi = \frac{\Delta}{\epsilon + m} = \frac{\epsilon - m}{\Delta^\dagger} \in \mathbb{H}. \tag{16}$$

Currently each component shows a 2×2 matrix, which takes a value in quaternion $\mathbb{H}$, so that the eigenvector is a 2×4 matrix due to the degeneracy, namely $\psi = (\psi_1 \; \psi_2)$, where each $\psi_{1,2}$ is a four vector. For a degenerated system, we can define non-Abelian analog of the Berry connection $\mathcal{A}_{ab} = \psi_a^\dagger (id) \psi_b$ for $a, b = 1, 2$. In this case, we obtain an SU(2) valued Berry connection, which is a consequence of S^3 fibration of $\mathbb{H}\mathbf{P}^1 = S^7 / S^3$. The topological invariant for the 4d system is given by the four-dimensional momentum integral of the second Chern class, which is known as the instanton number,

$$\nu_{4d} = -\frac{1}{8\pi^2} \int \mathrm{Tr}\mathcal{F} \wedge \mathcal{F} = \frac{1}{2} \mathrm{sign}(m). \tag{17}$$

Actually the instanton configuration obtained here, by solving a matrix equation, is closely related to the ADHM construction. See [12] for more details. We again obtain a half-integer topological invariant. The reason is totally parallel with the previous case. To obtain an integer valued topological invariant, we consider the 5d uplift, the 5d WSM, obtained by replacing the mass with another momentum $m \to p_5$,

$$\mathcal{H}_{5d}(p) = p \cdot \gamma + p_5 \gamma_5, \tag{18}$$

and thus the integral over the 5d momentum space, instead of 4d, gives rise to

$$\nu_{5d} = -\frac{1}{8\pi^2} \int_{S^4} \mathrm{Tr}\mathcal{F} \wedge \mathcal{F} = 1, \tag{19}$$

which implies the SU(2) monopole, called the Wu-Yang monopole, at the origin in the momentum space. Then the 4d momentum integral performed to obtain the 4d invariant ν_{4d} is equivalent to the hemisphere integral of S^4, which provides a half of the 5d invariant.

3. Boundary condition analysis

3.1. Operator formalism

In order to discuss the boundary condition, we start with a first order Hermitian differential operator [3, 4, 17, 18]

$$\widehat{D} = -i\sigma \frac{\partial}{\partial x}. \tag{20}$$

Now we put a Pauli matrix σ, but we can consider a generic Hermitian matrix. Considering the inner product in a finite size system defined on the interval $x \in [x_L, x_R]$, we obtain

$$
\begin{aligned}
\left\langle \phi \middle| \widehat{D}\psi \right\rangle &= \int_{x_L}^{x_R} dx\, \phi(x)^{\dagger} \left(-i\sigma \frac{\partial}{\partial x} \psi(x) \right) \\
&= \phi(x)^{\dagger}(-i\sigma)\psi(x) \Big|_{x_L}^{x_R} + \int_{x_L}^{x_R} dx \left(-i\sigma \frac{\partial}{\partial x} \phi(x) \right)^{\dagger} \psi(x) \\
&= \phi(x)^{\dagger}(-i\sigma)\psi(x) \Big|_{x_L}^{x_R} + \left\langle \widehat{D}\phi \middle| \psi \right\rangle.
\end{aligned}
\tag{21}
$$

The Hermitian condition $\left\langle \phi \middle| \widehat{D}\psi \right\rangle = \left\langle \widehat{D} \middle| \phi\psi \right\rangle$ implies that the surface term should vanish

$$\phi(x)^{\dagger}\sigma\psi(x) \Big|_{x_L}^{x_R} = \phi(x_R)^{\dagger}\sigma\psi(x_R) - \phi(x_L)^{\dagger}\sigma\psi(x_L) = 0, \tag{22}$$

which gives rise to two possibilities:

1. Periodic boundary condition: $\phi(x_R) = \phi(x_L)$ and $\psi(x_R) = \psi(x_L)$

2. Open boundary condition: $\phi(x_R)^{\dagger}\sigma\psi(x_R) = 0$ and $\phi(x_L)^{\dagger}\sigma\psi(x_L) = 0$

In particular, the open boundary condition 2 has the following solution

$$P\psi\big|_{x_{L,R}} = P\phi\big|_{x_{L,R}} = 0 \quad \text{where} \quad P = \frac{\mathbb{1} - M}{2} \tag{23}$$

with the matrix M satisfying $M^{\dagger}\sigma + \sigma M = 0$, since $\psi = M\psi$, $\phi = M\phi$ at the boundary, then

$$\phi^{\dagger}\sigma\psi = \phi^{\dagger}\sigma M\psi = -\phi^{\dagger}M^{\dagger}\sigma\psi = -\phi^{\dagger}\sigma\psi \quad \Rightarrow \quad \phi^{\dagger}\sigma\psi = 0. \tag{24}$$

In general we can apply different matrices $M_{L,R}$ for x_L and x_R, but here we assume $M_{L,R} = M$ for simplicity, namely the same boundary condition for $x_{L,R}$. We remark that the condition (23) is specific to the operator choice (20). We have to derive the corresponding boundary condition case by case. We will show a generic formulation of the boundary condition using the Lagrangian formalism in Section 3.2.

3.1.1. Lattice system

Let us apply the similar argument to the lattice system defined on a one-dimensional interval $n \in \{1, \dots, N\}$. We introduce an analogous difference operator to (20) as

$$\widehat{D}_{\text{lat}} = -i\sigma \nabla \tag{25}$$

where $\nabla \psi_n = \psi_{n+1} - \psi_n$ and $\nabla^{\dagger}\psi_n = \psi_{n-1} - \psi_n$. In this case, the inner product $\left\langle \phi \middle| \widehat{D}_{\text{lat}}\psi \right\rangle$ is given by

$$\sum_{n=1}^{N} \phi_n^\dagger \left(-i\sigma\nabla\psi_n \right) = \sum_{n=1}^{N} \left(i\sigma\nabla^\dagger\phi_n \right)^\dagger \psi_n + \phi_0^\dagger (i\sigma)\psi_1 - \phi_N^\dagger (i\sigma)\psi_{N+1} \tag{26}$$

where ϕ_0 and ψ_{N+1} are considered as auxiliary fields. The self-conjugacy condition $\left\langle \phi \big| \widehat{D}_{\mathrm{lat}} \psi \right\rangle = \left\langle \widehat{D}_{\mathrm{lat}} \phi \big| \psi \right\rangle$ requires that the surface term should vanish:

$$\phi_0^\dagger \sigma \psi_1 - \phi_N^\dagger \sigma \psi_{N+1} = 0. \tag{27}$$

The periodic boundary condition $\phi_{n+N} = \phi_n$, $\psi_{n+N} = \psi_n$ is a simple solution to this. The other possibility is that each term independently vanishes, corresponding to the open boundary condition. This means that the lattice system is similarly considered as the continuum system, and the open boundary condition is imposed by (23). We remark that for the lattice system the surface term (27) is not given by the on-site term, but involving a hopping to the next site. This suggests that we have to take care of the locality and continuum limit of the system.

3.1.2. Example

Let us consider an example with $\sigma = \sigma_3$. Then the matrix M should be a linear combination of $\sigma_{1,2}$. Since the operator P has a zero eigenvalue, the determinant should vanish $\det P = 0$, which leads to

$$M = \sigma_1 \cos\theta + \sigma_2 \sin\theta = \begin{pmatrix} 0 & e^{-i\theta} \\ e^{i\theta} & 0 \end{pmatrix}, \tag{28}$$

obeying $M^\dagger = M$ and $M^2 = \mathbb{1}$ with two eigenvalues ± 1. It is also expressed as $M = \sigma_1 e^{i\theta\sigma_3} = \sigma_2 e^{i\left(\theta - \frac{\pi}{2}\right)\sigma_3}$. Thus the operator $P(= P^\dagger)$ turns out to be a projection operator $P^2 = P$ having eigenvalues $1, 0$ with the corresponding eigenvectors

$$P\begin{pmatrix} 1 \\ -e^{i\theta} \end{pmatrix} = \begin{pmatrix} 1 \\ -e^{i\theta} \end{pmatrix} \quad \text{and} \quad P\begin{pmatrix} 1 \\ e^{i\theta} \end{pmatrix} = 0. \tag{29}$$

We remark $\sigma_3 P = \breve{P}\sigma_3$, $\sigma_3\breve{P} = P\sigma_3$ where $\breve{P} = \mathbb{1} - P$ obeying $\breve{P}P = P\breve{P} = 0$. Thus we obtain a one-parameter family of the solution to the boundary condition (23),

$$\psi\big|_{x_{L,R}} \propto \begin{pmatrix} 1 \\ e^{i\theta} \end{pmatrix}. \tag{30}$$

Since $\breve{P}\psi = \psi$, the current in x_3-direction vanishes at the boundary, $J_3 = \psi^\dagger \sigma_3 \psi = \psi^\dagger \breve{P}\sigma_3 \breve{P}\psi = \psi^\dagger \sigma_3 P\breve{P}\psi = 0$. In other words, the open boundary condition is interpreted as a vanishing condition for the normal component of the current as expected.

3.2. Lagrangian formalism

We explain how to derive a proper boundary condition for a given system with the Lagrangian formalism. The integral over the spacetime $\mathcal{M}$ of the Lagrangian defines the action

$$S = \int_{\mathcal{M}} \mathcal{L}(\phi, \partial\phi). \tag{31}$$

If the system has a continuous local symmetry, the action may be invariant under the infinitesimal deviation of the field $\phi \rightarrow \phi + \epsilon(x)\varphi^3$:

$$0 = \delta S$$

$$= \int_{\mathcal{M}} \left(\frac{\partial\mathcal{L}}{\partial\phi} - \partial_\mu \left(\frac{\partial\mathcal{L}}{\partial(\partial_\mu\phi)} \right) \right) \epsilon(x)\varphi - \int_{\mathcal{M}} \epsilon(x)\partial_\mu \left(\frac{\partial\mathcal{L}}{\partial(\partial_\mu\phi)} \varphi \right) + \int_{\mathcal{M}} \partial_\mu \left(\frac{\partial\mathcal{L}}{\partial(\partial_\mu\phi)} \epsilon(x)\varphi \right). \tag{32}$$

The first term vanishes due to the Euler-Lagrange equation of motion for the bulk, $\frac{\partial\mathcal{L}}{\partial\phi} - \partial_\mu \left(\frac{\partial\mathcal{L}}{\partial(\partial_\mu\phi)} \right) = 0$. The vanishing condition for the second term implies the current $J^\mu = \frac{\partial\mathcal{L}}{\partial(\partial_\mu\phi)}\varphi$, satisfying the conservation law $\partial_\mu J^\mu = 0$, a.k.a. the Nöther current. The third term is a surface contribution which plays a role in the system with the boundary. The invariance of the action is thus rephrased as

$$0 = \int_{\partial\mathcal{M}} \epsilon(x) n \cdot J \tag{33}$$

where n is the normal vector defined as $\int_{\mathcal{M}} \partial_\mu V^\mu = \int_{\partial\mathcal{M}} n \cdot V$ with an arbitrary vector field V^μ and the boundary of the manifold denoted by $\partial\mathcal{M}$. This ends up with the condition such that the normal component of the current should vanish at the boundary

$$n \cdot J \Big|_{\partial\mathcal{M}} = 0. \tag{34}$$

This seems physically reasonable and consistent with the previous argument in Section 3.1.2 because at the boundary there is no ingoing and outgoing current.

Furthermore, this zero current condition can be modified by taking into account the additional surface contribution to the action

$$S_B = \int_{\partial\mathcal{M}} \mathcal{L}_B(\phi) \tag{35}$$

where we assume the boundary d.o.f. is not dynamical (not including the derivative $\partial\phi$). Then the condition (34) becomes

$$\left[n \cdot J + \frac{\partial\mathcal{L}_B}{\partial\phi}\varphi \right]_{\partial\mathcal{M}} = 0. \tag{36}$$

This characterizes the boundary condition. In the following, we consider several examples to see how the boundary condition plays a role in the topological materials.

---

[3]This is an assumption. In general, the action itself is not invariant under the deviation.

3.3. 3d Weyl semimetal

3.3.1. Continuum system

Let us apply the argument discussed above to the WSM system. We consider the effective Hamiltonian (6) with a slight modification

$$\mathcal{H}_{3d}\left(\vec{p}, x_3\right) = p_1\sigma_1 + p_2\sigma_2 - i\sigma_3\frac{\partial}{\partial x_3}. \tag{37}$$

We put a boundary only at $x_3 = 0$ for simplicity, so that the system is defined on a positive domain $x_3 > 0$. In this case, since the current operator is defined as $\vec{J} = \psi^\dagger\,\vec{\sigma}\,\psi$, the boundary condition, corresponding to the zero current condition (36), that we impose is[4]

$$\psi^\dagger\sigma_3\psi\Big|_{x_3=0} = 0. \tag{38}$$

The eigenstate satisfying the condition (38) is parameterized by a single phase factor

$$\psi\left(\vec{p}, x_3\right) = \sqrt{\alpha\left(\vec{p}\right)}e^{-\alpha\left(\vec{p}\right)x_3}\begin{pmatrix} 1 \\ e^{i\theta} \end{pmatrix} \tag{39}$$

which is normalized as $\int_0^\infty dx_3\,\psi^\dagger\psi = 1$, and the normalizability requires $\alpha\left(\vec{p}\right) > 0$. This eigenstate is localized on the boundary $x_3 = 0$ and exponentially decay into the bulk $x_3 > 0$ due to the factor $e^{-\alpha\left(\vec{p}\right)x_3}$, where the parameter $\alpha\left(\vec{p}\right)$ plays a role as the inverse penetration length. In this case, the exponential factor $e^{-\alpha\left(\vec{p}\right)x_3}$ is responsible for the x_3-direction dependence, instead of the plane wave factor $e^{ip_3x_3}$ used for the bulk analysis. In other words, the current analysis of the edge state uses Laplace basis instead of Fourier basis. Therefore, under the replacement $p_3 \to i\alpha$, we can apply almost the same analysis.

Then the spectrum and the inverse penetration length of the edge state are obtained from the eigenvalue equation, given as follows

$$\epsilon\left(\vec{p}\right) = p_1\cos\theta + p_2\sin\theta, \qquad \alpha\left(\vec{p}\right) = -p_1\sin\theta + p_2\cos\theta. \tag{40}$$

Actually it is written using an SO(2) transformation with the relation $\epsilon^2 + \alpha^2 = \left|\vec{p}\right|^2$,

$$\begin{pmatrix} \epsilon \\ \alpha \end{pmatrix} = \begin{pmatrix} \cos\theta & \sin\theta \\ -\sin\theta & \cos\theta \end{pmatrix}\begin{pmatrix} p_1 \\ p_2 \end{pmatrix}. \tag{41}$$

We show the spectrum of the edge state depending on the boundary condition with the bulk spectrum in **Figure 6**. We remark that the edge state cannot be defined in the whole

---

[4]This is of course equivalent to the boundary condition discussed in Section 3.1.2.

momentum space due to the normalizability condition $\alpha\left(\vec{p}\right) > 0$. Such a bounded spectrum associated with the WSM edge state is called the Fermi arc, and the boundary condition parameter, a relative phase factor, parameterizes the direction of the arc. Accordingly the current similarly behaves as $(J_1, J_2, J_3) \propto (\cos\theta, \sin\theta, 0)$.

3.3.2. Lattice system

Let us apply a similar analysis to the lattice model for 3d WSM. We consider the lattice model (13) with a boundary at $n_3 = 1$, defined on the positive n_3 region, $n_3 \geq 1$,

$$\mathscr{H}_{3d}^{lat}\left(\vec{p}, n_3\right) = \begin{pmatrix} 0 & \Delta\left(\vec{p}\right)^* \\ \Delta\left(\vec{p}\right) & 0 \end{pmatrix} - \frac{i}{2}\sigma_3\left(\nabla_3 - \nabla_3^\dagger\right) \tag{42}$$

with a complex parameter

$$\Delta\left(\vec{p}\right) = \cos p_1 - \cos p_2 + c + i \sin p_2, \tag{43}$$

which is analogous to the model in the continuum $\Delta\left(\vec{p}\right) \sim p_1 \pm i p_2$. We keep an explicit n_3-dependence of the system to deal with the boundary condition. According to the discussion in Sections 3.1.1 and 3.1.2, we consider the edge state consistent with the boundary condition as

$$\psi\left(\vec{p}, n_3\right) = \beta\left(\vec{p}\right)^{n_3-1}\begin{pmatrix} 1 \\ e^{i\theta} \end{pmatrix} \tag{44}$$

where $\beta\left(\vec{p}\right)$ is a real parameter, corresponding to the penetration depth, and the normalizability requires $|\beta\left(\vec{p}\right)| < 1$. In particular, we consider the situation $0 < \beta\left(\vec{p}\right) < 1$ for the moment: The negative $\beta\left(\vec{p}\right)$ solution is interpreted as a doubling counterpart of the positive one. The eigenvalue equation $\mathscr{H}_{3d}^{lat}\left(\vec{p}, n_3\right)\psi\left(\vec{p}, n_3\right) = \epsilon\left(\vec{p}\right)\psi\left(\vec{p}, n_3\right)$ leads to
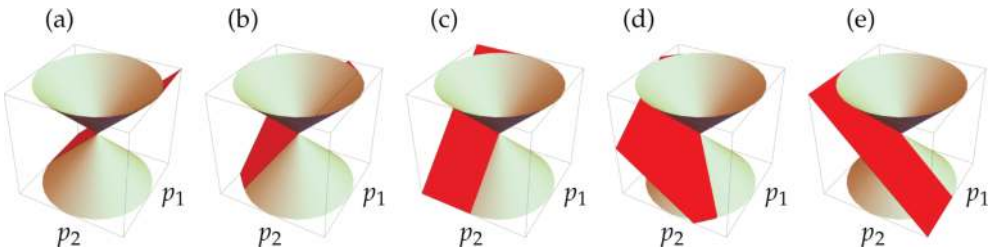

Figure 6. The boundary condition dependence of the edge state spectrum for $\theta = 0, \pi/4, \pi/2, 3\pi/4, \pi$ with the bulk spectrum. The parameter θ plays a role as a rotation angle in the momentum space.

$$\mathcal{D}\psi\left(\vec{p},n_3\right) = 0 \quad \text{with} \quad \mathcal{D} = \begin{pmatrix} i\tilde{\alpha}\left(\vec{p}\right) - \epsilon\left(\vec{p}\right) & \Delta\left(\vec{p}\right)^* \\ \Delta\left(\vec{p}\right) & -i\tilde{\alpha}\left(\vec{p}\right) - \epsilon\left(\vec{p}\right) \end{pmatrix} \tag{45}$$

where we define $\tilde{\alpha}\left(\vec{p}\right) = \frac{\beta(\vec{p})^{-1} - \beta(\vec{p})}{2}$. Since we consider the situation $0 < \beta\left(\vec{p}\right) < 1$, it turns out $\tilde{\alpha}\left(\vec{p}\right) > 0$. The solution is then obtained as

$$\epsilon\left(\vec{p}\right) = \cos\theta \operatorname{Re}\Delta\left(\vec{p}\right) + \sin\theta \operatorname{Im}\Delta\left(\vec{p}\right) \tag{46}$$

$$\tilde{\alpha}\left(\vec{p}\right) = -\sin\theta \operatorname{Re}\Delta\left(\vec{p}\right) + \cos\theta \operatorname{Im}\Delta\left(\vec{p}\right) \tag{47}$$

which has an analogous expression as (41) using SO(2) rotation

$$\begin{pmatrix} \epsilon \\ \tilde{\alpha} \end{pmatrix} = \begin{pmatrix} \cos\theta & \sin\theta \\ -\sin\theta & \cos\theta \end{pmatrix} \begin{pmatrix} \operatorname{Re}\Delta \\ \operatorname{Im}\Delta \end{pmatrix}. \tag{48}$$

At this moment, it is obvious that the spectrum of the current lattice model is parallel with the continuum model under the correspondence $(p_1, p_2, \alpha) \leftrightarrow (\operatorname{Re}\Delta, \operatorname{Im}\Delta, \tilde{\alpha})$.

We show the spectrum of the edge state in **Figure 7**, in particular, its boundary condition dependence. **Figure 8** shows constant energy slices of the spectrum. We can see the so-called Fermi arc, which connects two bulk Weyl points. As discussed for the continuum model, the boundary condition parameter plays a role as a rotation angle in the momentum space.

3.4. 2d topological insulator

3.4.1. Continuum system

The 2d class A TI is given by the dimensional reduction of the 3d WSM. Replacing $p_2 \to m$ in the Hamiltonian (37), we obtain
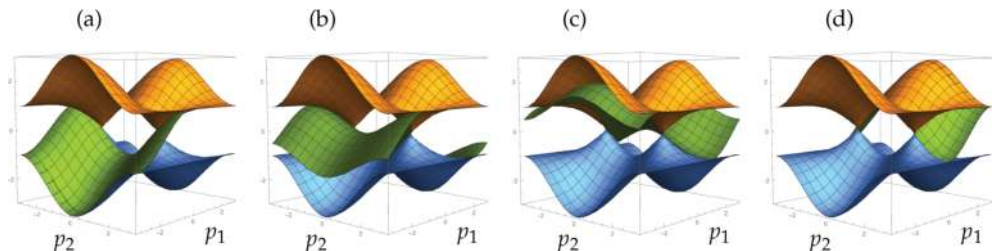

Figure 7. The boundary condition dependence of the edge state spectrum $\epsilon\left(\vec{p}\right)$ for $\theta = \pi 4, \pi/3, 5\pi/3, 2\pi$ (green), in addition to the bulk spectrum (orange and blue), the parameter c is taken to be $c = 1$.
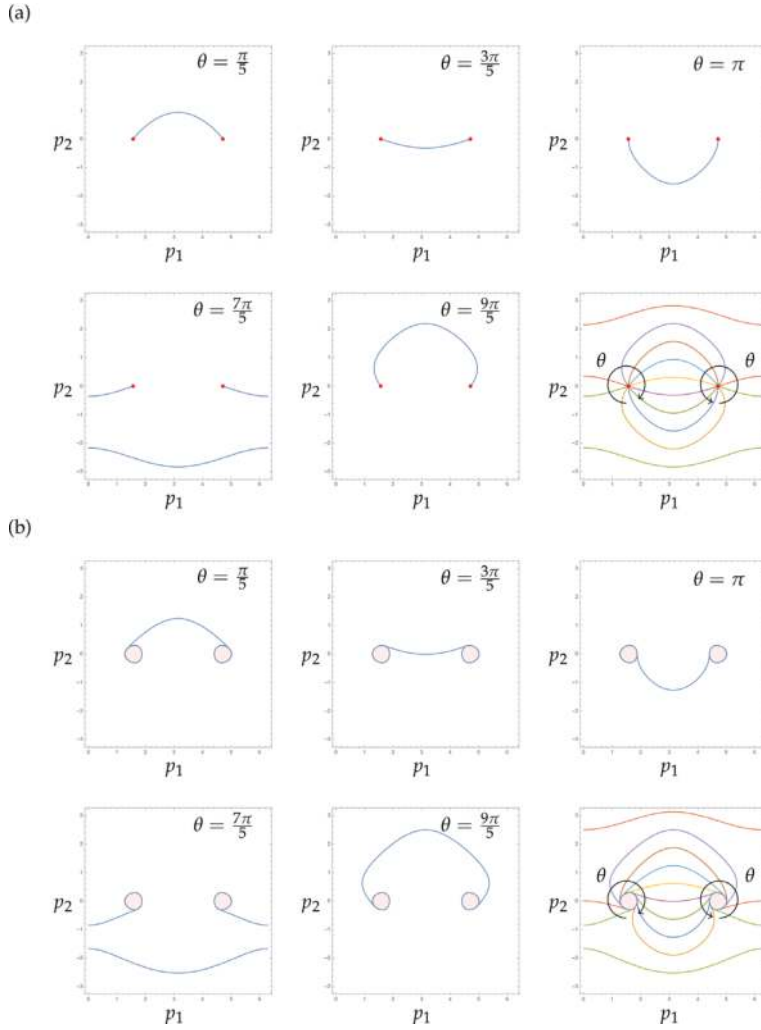
Figure 8. The Fermi arc at (a) zero energy $\varepsilon\left(\vec{p}\right) = 0$ and (b) finite energy $\epsilon\left(\vec{p}\right) = 0.3$ with $\theta = \pi/5, 3\pi/5, \pi, 7\pi/5, 9\pi/5$. The red dot and shaded region show the bulk contribution. The last panels show Fermi arcs with various values of the parameter θ.

$$\mathscr{H}_{2\mathrm{d}}\left(p_1, x_3\right) = p_1\sigma_1 + m\sigma_2 - i\sigma_3\frac{\partial}{\partial x_3}. \tag{49}$$

After this dimensional reduction, we can apply totally the same analysis to this model discussed in Section 3.3: we consider the localized edge state satisfying the boundary condition

$$\psi(p_1, x_3) = \sqrt{\alpha(p_1)} e^{-\alpha(p_1) x_3} \begin{pmatrix} 1 \\ e^{i\theta} \end{pmatrix} \tag{50}$$

where the inverse penetration depth $\alpha(p_1)$ has to be positive due to the normalizability. Then we obtain the solution

$$\epsilon(p_1) = p_1 \cos\theta + m \sin\theta, \qquad \alpha(p_1) = -p_1 \sin\theta + m \cos\theta. \tag{51}$$

Figure 9 shows the boundary condition dependence of the edge state spectrum. Replacement $p_2 \to m$ corresponds to take a section at $p_2 = m$, and the 3d Fermi arc is reduced to the 2d chiral edge mode.

3.4.2. Lattice system

Similarly, we consider the dimensional reduction of the lattice Hamiltonian of 3d WSM (13). In this case, we have two options,

$$p_1 \to m_1: \quad \mathcal{H}_{2d}^{(1)} = \sigma_1 \big(\cos m_1 - \cos p_2 + c\big) + \sigma_2 \sin p_2 + \sigma_3 \sin p_3 \tag{52}$$

$$p_2 \to m_2: \quad \mathcal{H}_{2d}^{(2)} = \sigma_1 \big(\cos p_1 - \cos m_2 + c\big) + \sigma_2 \sin m_2 + \sigma_3 \sin p_3 \tag{53}$$

and the corresponding spectra are given as follows:

$$\epsilon_1(p_2, p_3) = \pm\sqrt{\big(\cos m_1 - \cos p_2 + c\big)^2 + \big(\sin p_2\big)^2 + \big(\sin p_3\big)^2} \tag{54}$$

$$\epsilon_2(p_1, p_3) = \pm\sqrt{\big(\cos p_1 - \cos m_2 + c\big)^2 + \big(\sin m_2\big)^2 + \big(\sin p_3\big)^2} \tag{55}$$
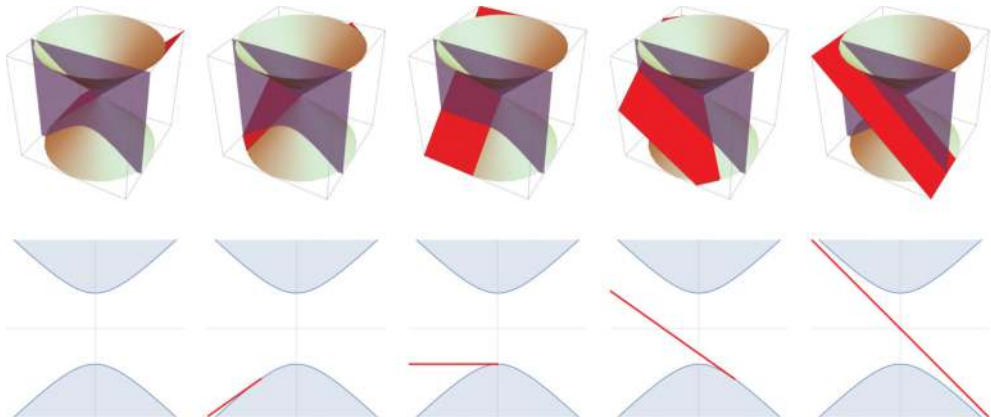

Figure 9. The boundary condition dependence of the edge state for the 2d system. The dimensional reduction corresponds to taking a section at $p_2 = m$. The horizontal axis in the bottom panel shows the momentum p_1.

We can follow the analysis discussed in Section 3.3.2 for the current system. **Figure 10** shows the boundary condition dependence of the edge state spectrum. These behaviors are consistent with the continuum model in the vicinity of the would-be gapless points. Such a dependence of the boundary condition has been recently predicted to be observed in monolayer silicene/germanene/stanene nanoribbons [19]. We remark that we obtain the edge state with positive and negative chiralities from the reduction $p_1 \rightarrow m_1$, which is equivalent to topologically trivial state. Actually the edge state is almost embedded, and indistinguishable with the bulk spectrum, in particular, for $\theta = 5\pi/7, 9\pi/7$. On the other hand, we obtain a single chiral edge state from the reduction $p_2 \rightarrow m_2$, indicating topologically nontrivial state. We can see an edge state spectrum survives for the whole region of the parameter θ.
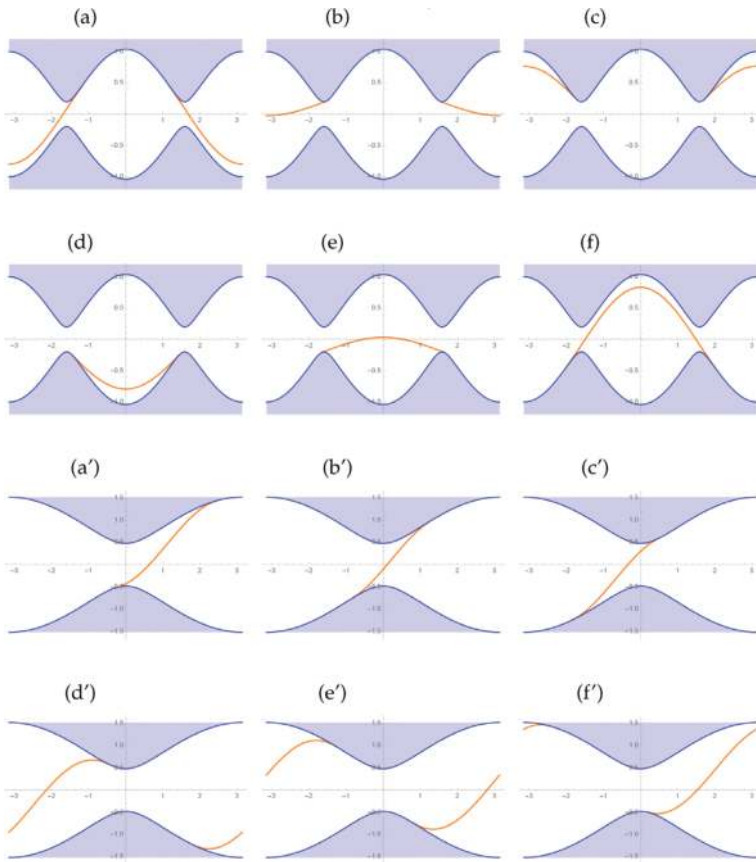

Figure 10. The boundary condition dependence of the 2d lattice system (52) and (53) with $c = 1$. (a)–(f) and (a′)–(f′) show the spectra obtained from the reduction $p_1 \rightarrow m_1 = \pi/2 + 0.5$ and $p_2 \rightarrow m_2 = 0.2$. The horizontal axes are the momenta p_2 and p_1, respectively. The blue region is the bulk, and the orange line is the edge state spectrum.

4. Edge-of-edge state

So far we have examined situations with a single boundary with the boundary condition. In general we can impose another boundary in the different direction, and a different boundary condition. In this section we consider a generic situation involving two boundaries with two different conditions. Then an intersection of two boundary plays a role of "edge-of-edge" and we study the corresponding edge-of-edge state localized on such an intersecting boundaries [4]. See also related works [20–24].

4.1. 5d Weyl semimetal

As discussed in Section 3.1, the boundary condition is characterized by the projection (23), so that the degrees of freedom of the boundary state should be a half of the original one. This implies that, if we impose two boundary conditions, we will have a quarter of the original d.o.f. Therefore, to obtain physical degrees of freedom at the edge-of-edge, we have to start with a four-component system or more. For this purpose, we start with the 5d WSM system discussed in Section 2.4 by introducing boundaries at $x_4 = 0$ and $x_5 = 0$. The boundary condition, namely the zero current condition (34), is now given by

$$\psi^\dagger \gamma_4 \psi \Big|_{x_4=0} = 0 \qquad \psi^\dagger \gamma_5 \psi \Big|_{x_5=0} = 0, \tag{56}$$

since the current operator is given by $J_\mu = \psi^\dagger \gamma_\mu \psi$. These conditions are rephrased as

$$P_4 \psi \Big|_{x_4=0} = 0 \quad P_5 \psi \Big|_{x_5=0} = 0 \quad \text{with} \quad P_{4,5} = \frac{\mathbb{1} - M_{4,5}}{2} \tag{57}$$

where the matrix $M_{4,5}$ obeys $M_a^\dagger \gamma_a + \gamma_a M_a = 0$ for $a = 4, 5$. Explicitly we have

$$M_5 = \begin{pmatrix} 0 & U_5^\dagger \\ U_5 & 0 \end{pmatrix}, \qquad M_4 = -\frac{1}{2} \begin{pmatrix} U_4 + U_4^\dagger & U_4 - U_4^\dagger \\ -U_4 + U_4^\dagger & -U_4 - U_4^\dagger \end{pmatrix}, \tag{58}$$

where $U_{4,5}$ are elements of U(2). A solution to these conditions localized at the boundary is given by

$$\psi\left(p_{1,2,3,5}, x_4\right) = e^{-\alpha_4(p)x_4} \begin{pmatrix} \mathbb{1} - U_4 \\ \mathbb{1} + U_4 \end{pmatrix} \chi\left(p_{1,2,3,4}\right), \quad \psi\left(p_{1,2,3,4}, x_5\right) = e^{-\alpha_5(p)x_5} \begin{pmatrix} \mathbb{1} \\ U_5 \end{pmatrix} \xi\left(p_{1,2,3,4}\right). \tag{59}$$

In particular, the edge state localized at $x_5 = 0$ is apparently similar to the 3d case (39), just replacing the phase factor $e^{i\theta} \in$ U(1) with $U_5 \in$ U(2). The eigenvalue equation $\mathcal{H}_{5d}\psi = \epsilon\psi$ leads to $\epsilon_5^2 + \alpha_5^2 = \left|\vec{p}\right|^2 + p_4^2$ and also

$$\left[(i\alpha_5 - \epsilon_5) + \left(p_4 - i\,\vec{\sigma}\cdot\vec{p}\right)U_5\right]\xi = 0. \tag{60}$$

Decomposing $U_5 = e^{i\theta_5}V_5$ with $e^{i\theta_5} \in$ U(1) and $V_5 \in$ SU(2), we consider the SU(2) transformation $\left(p_4 - i\,\vec{\sigma}\cdot\vec{p}\right)V_5 = p_4' - i\,\vec{\sigma}\cdot\vec{p}'$. Then we have

$$\left(\alpha_5\sin\theta_5 - \epsilon_5\cos\theta_5 + p_4'\right)\xi = 0, \tag{61}$$

$$\left(\alpha_5\cos\theta_5 + \epsilon_5\sin\theta_5 - \vec{\sigma}\cdot\vec{p}'\right)\xi = 0. \tag{62}$$

Diagonalizing $\vec{\sigma}\cdot\vec{p}'$, which is equivalent to the 3d Hamiltonian (6), as $\left(\vec{\sigma}\cdot\vec{p}'\right)\xi_\pm = \pm\sqrt{\left|\vec{p}'\right|^2}\xi_\pm$, we obtain the spectrum and the inverse penetration depth as follows:

$$\epsilon_5(p) = p_4'\cos\theta_5 \pm \sqrt{\left|\vec{p}'\right|^2}\sin\theta_5, \qquad \alpha_5(p) = -p_4'\sin\theta_5 \pm \sqrt{\left|\vec{p}'\right|^2}\cos\theta_5, \tag{63}$$

which is written using an SO(2) transformation as before,

$$\begin{pmatrix}\epsilon_5 \\ \alpha_5\end{pmatrix} = \begin{pmatrix}\cos\theta_5 & \sin\theta_5 \\ -\sin\theta_5 & \cos\theta_5\end{pmatrix}\begin{pmatrix}p_4' \\ \pm\sqrt{\left|\vec{p}'\right|^2}\end{pmatrix}. \tag{64}$$

We can solve the boundary condition and obtain the spectrum for the boundary at $x_4 = 0$ in a similar way.

Let us then consider a compatible boundary condition for the localized edge-of-edge state

$$P_4\psi\Big|_{x_{4,5}=0} = P_5\psi\Big|_{x_{4,5}=0} = 0. \tag{65}$$

A solution to this condition is given by

$$\psi\left(p_{1,2,3}, x_4, x_5\right) = e^{-\alpha_4(p)x_4 - \alpha_5(p)x_5}\begin{pmatrix}\mathbb{1} - U_4 \\ \mathbb{1} + U_4\end{pmatrix}\chi(p) \tag{66}$$

with $[U_5(\mathbb{1} - U_4) - (\mathbb{1} + U_4)]\chi(p) = 0$, which is covariant under U(2) transformation $(U_4, U_5, \chi) \to \left(WU_4W^\dagger, WU_5W^\dagger, W\chi\right)$ with $W \in$ U(2). To have a nontrivial solution, they should obey $[U_5(\mathbb{1} - U_4) - (\mathbb{1} + U_4)] = 0$. For example, a simple choice is $(U_4, U_5) = (\sigma_3, \sigma_2)$, and the corresponding solution is $\chi^T = (1\ i)$. Then we obtain the spectrum of the edge-of-edge state $\epsilon(p) = -p_1$, $\alpha_4(p) = p_3$, $\alpha_5(p) = p_2$.

4.2. 3d chiral topological insulator

We discuss dimensional reduction of the edge-of-edge state in the 5d WSM to a more realistic 3d system. Replacing $(p_4, p_5) \to (m, 0)$ as shown in **Figure 11**, then we obtain the 3d chiral (class AIII) TI

$$\mathcal{H}_{3d}^{AIII}\left(\vec{p}\right) = \vec{p}\cdot\vec{\gamma} + m\gamma_4, \tag{67}$$

where the gamma matrices are chosen as $\vec{\gamma} = \tau_2\otimes\vec{\sigma}$, $\gamma_4 = \tau_1\otimes\mathbb{1}$, $\gamma_5 = \tau_3\otimes\mathbb{1}$, and Pauli matrices $\sigma's$ and $\tau's$ act on the spin space $(\uparrow,\downarrow)$ and the sublattice space (A, B), respectively. This Hamiltonian has a chiral symmetry with respect to the sublattice structure $\{\mathcal{H}_{3d}^{AIII},\gamma_5\} = 0$. We can apply a similar analysis as before. The edge-of-edge state is in this case given by

$$\psi(p_1, x_2, x_3) = e^{-\alpha_2(p_1)x_2 - \alpha_3(p_1)x_3}\begin{pmatrix} \mathbb{1} + i\sigma_3 U_3 \\ i\sigma_3(\mathbb{1} - i\sigma_3 U_3) \end{pmatrix}\xi(p_1) \tag{68}$$

with the compatibility condition

$$\det\left[\mathbb{1} + U_2^\dagger(i\sigma_2) + i\sigma_3 U_3 - U^\dagger(i\sigma_1)U_3 + i\sigma_1 - i\sigma_2 U_3 - U_2^\dagger(i\sigma_3) - U_2^\dagger U_3\right] = 0 \tag{69}$$

where $U_{2,3}\in$ U(2) parameterize the boundary condition. We consider the following choice satisfying the compatibility condition $U_2 = \sigma_2\cos\phi + i\sin\phi$, $U_3 = i\cos\phi - \sigma_3\sin\phi$. Then we obtain the spectra of the edge state localized at $x_2 = 0$ and x_3, and the edge-of-edge state localized at their intersection

$$\epsilon_2(p_1, p_3) = \pm\sqrt{p_1^2 + p_3^2 + (m\cos\phi)^2}, \tag{70}$$

$$\epsilon_3(p_1, p_2) = \pm\sqrt{p_1^2 + p_2^2 + (m\sin\phi)^2}, \tag{71}$$

$$\epsilon_{eoe}(p_1) = -p_1. \tag{72}$$

Here both edge states are gapped, while only the edge-of-edge state is gapless. This is a suitable situation for experimental detection of the edge-of-edge state because we have to distinguish it from the spectra of the edge states at $x_2 = 0$ and $x_3 = 0$. The reason why we obtain the gapped edge states seems that the symmetry protecting the edge state is weakly broken due to the boundary condition, which is analogous to the TI/ferromagnet junction, etc.
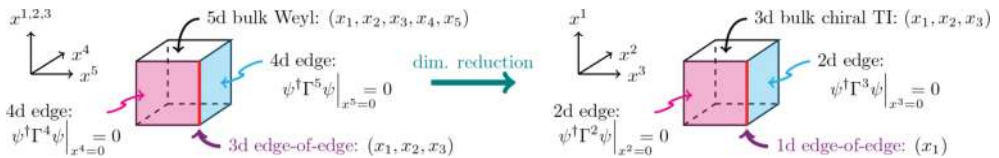

Figure 11. Dimensional reduction from 5d WSM to 3d chiral TI. There exists the edge-of-edge state localized at the boundary intersection, propagating in x_1-direction.

Acknowledgements

Author details

Taro Kimura

Address all correspondence to: taro.kimura@keio.jp

Department of Physics, Keio University, Japan

References

[1] Hasan MZ, Kane CL. Topological insulators. Reviews of Modern Physics. 2010;**82**:3045

[2] Wen X-G. Quantum Field Theory of Many-Body Systems: From the Origin of Sound to an Origin of Light and Electrons. Oxford: Oxford University Press; 2004

[3] Hashimoto K, Kimura T, Wu X. Boundary conditions of Weyl semimetals. Progress of Theoretical and Experimental Physics. 2017;**2017**:053I01

[4] Hashimoto K, Kimura T, Wu X. Edge states at an intersection of edges of a topological material. Physics Review. 2017;**B95**:165443

[5] Devizorova ZA, Volkov VA. Fermi arcs formation in Weyl semimetals: The key role of intervalley interaction. Physics Review. 2016;**B95**:081302(R)

[6] Enaldiev VV, Zagorodnev IV, Volkov VA. Boundary conditions and surface states spectra in topological insulators. JETP Letters. 2015;**101**:89-96

[7] Isaev L, Moon YH, Ortiz G. Bulk-boundary correspondence in three-dimensional topological insulators. Physics Review. 2011;**B84**:075444

[8] Kitaev AY. Periodic table for topological insulators and superconductors. AIP Conference Proceedings. 2009;**1134**:22-30

[9] Schnyder AP, Ryu S, Furusaki A, Ludwig AWW. Classification of topological insulators and superconductors in three spatial dimensions. Physics Review. 2008;**B78**:195125

[10] Chruściński D, Jamiołkowski A. Geometric phases in classical and quantum mechanics. In: Progress in Mathematical Physics. Vol. 36. Boston: Birkhäuser; 2004

[11] Thouless DJ, Kohmoto M, Nightingale MP, den Nijs M. Quantized Hall conductance in a two-dimensional periodic potential. Physical Review Letters. 1982;**49**:405-408

[12] Hashimoto K, Kimura T. Band spectrum is D-brane. Progress of Theoretical and Experimental Physics. 2016;**2016**:013B04

[13] Kimura T. Domain-wall, overlap, and topological insulators. PoS Lattice. 2016;**2015**:042

[14] Golterman MFL, Jansen K, Kaplan DB. Chern-Simons currents and chiral fermions on the lattice. Physics Letters. 1993;**B301**:219-223

[15] Nielsen HB, Ninomiya M. Absence of neutrinos on a lattice. 1. Proof by Homotopy theory. Nuclear Physics. 1981a;**B185**:20-40

[16] Nielsen HB, Ninomiya M. Absence of neutrinos on a lattice. 2. Intuitive topological proof. Nuclear Physics. 1981b;**B193**:173-194

[17] Hashimoto K, Kimura T. Topological number of edge states. Physics Review. 2016b;**B93**: 195166

[18] Witten E. Three lectures on topological phases of matter. La Rivista del Nuovo Cimento. 2016;**39**:313-370

[19] Hattori A, Tanaya S, Yada K, Araidai M, Sato M, Hatsugai Y, Shiraishi K, Tanaka Y. Edge states of hydrogen terminated monolayer materials: Silicene, germanene and stanene ribbons. Journal of Physics: Condensed Matter. 2017;**29**:115302

[20] Benalcazar WA, Bernevig BA, Hughes TL. Electric multipole moments, topological pumping, and a chiral hinge insulator. Physics Review. 2017;**B96**:245115

[21] Benalcazar WA, Bernevig BA, Hughes TL. Quantized electric multipole insulators. Science. 2017;**357**:61-66

[22] Langbehn J, Peng Y, Trifunovic L, von Oppen F, Brouwer PW. Reflection-symmetric second-order topological insulators and superconductors. Physical Review Letters. 2017; **119**:246401

[23] Schindler F, Cook AM, Vergniory MG, Wang Z, Parkin SSP, Bernevig BA, Neupert T. Higher-Order Topological Insulators. 2017;arXiv:1708.03636

[24] Song Z, Fang Z, Fang C. (d-2)-dimensional edge states of rotation symmetry protected topological states. Physical Review Letters. 2017;**119**:246402